

# Simple dynamical models of the Sagittarius dwarf galaxy

Amina Helmi<sup>1</sup> and Simon D.M. White<sup>2</sup>

<sup>1</sup> *Sterrewacht Leiden, Postbus 9513, 2300 RA Leiden, The Netherlands*

<sup>2</sup> *Max-Planck-Institut für Astrophysik, Karl-Schwarzschild-Str. 1, 85740 Garching bei München, Germany*

Accepted ... Received ...; in original form ...

## ABSTRACT

We present two simple dynamical models for Sagittarius based on N-body simulations of the progressive disruption of a satellite galaxy orbiting for 12.5 Gyr within a realistic Galactic potential. In both models the satellite initially has observable properties similar to those of current outlying dwarfs; in one case it is purely stellar while in the other it is embedded in an extended massive halo. The purely stellar progenitor is a King model with a total velocity dispersion of  $18.1 \text{ km s}^{-1}$ , a core radius of 0.56 kpc and a tidal radius of 3.8 kpc. The initial stellar distribution in the other case follows a King profile with the same core radius, a similar total velocity dispersion and a smaller extent. Both these models are consistent with all published data on the current Sagittarius system, they match not only the observed properties of the main body of Sagittarius, but also those reported for unbound debris at larger distances.

**Key words:** galaxies: interactions, individual (Sagittarius dSph)

## 1 INTRODUCTION

The Sagittarius dwarf galaxy is the closest satellite of the Milky Way (Ibata, Gilmore & Irwin 1994, 1995, hereafter IGI95). Soon after its discovery, several groups carried out simulations to see if its properties are consistent with the disruption of an object similar to the other dwarf companions of the Milky Way, but none produced a model in full agreement with both the age and the structure of the observed system (Johnston, Spiegel & Hernquist 1995; Velázquez & White 1995; Edelson & Elmegreen 1997; Ibata et al. 1997, hereafter I97). All groups assumed light to trace mass and an initial system similar to observed dwarf spheroidals. All found the simulated galaxy to disrupt after one or two orbits whereas the observed system has apparently completed ten or more. Most considered this to be a problem (but cf Velázquez & White 1995). As a result, several unconventional models were proposed to explain the survival and structure of Sagittarius. In an extensive numerical study, Ibata & Lewis (1998) concluded that Sagittarius must have a rigid and extended dark matter halo if it is to survive with 25% of its initial mass still bound today. Since an extended halo cannot remain undistorted in the Galaxy’s tidal field for any conventional form of dark matter, it is unclear how this idea should be interpreted. Furthermore, it produces an uncomfortably large mass-to-light ratio ( $\sim 100$ ), it cannot reproduce the observed elongation, and it suggests that little tidal debris will be liberated, in apparent conflict with the observations of Mateo, Olszewski & Morrison (1998), and Majewski et al. (1999) (see also Johnston et al. 1999). A somewhat less unorthodox model was proposed by

**Table 1.** Properties of Sagittarius (IGI95, I97)

| Orbital properties                                      |                                    |
|---|------------------------------------|
| distance from the Sun $d$                               | $25 \pm 2 \text{ kpc}$             |
| heliocentric radial velocity $v_r^{\text{sun}}$         | $140 \pm 2 \text{ km s}^{-1}$      |
| proper motion in $b$ $\mu_b$                            | $250 \pm 90 \text{ km s}^{-1}$     |
| gradient along the orbit $dv_r/db$                      | $< 3 \text{ km s}^{-1}/\text{deg}$ |
| angular position in the sky $(l, b)$                    | $(5.6^\circ, -14^\circ)$           |
| Internal properties                                     |                                    |
| luminosity  | $\gtrsim 10^7 L_\odot$             |
| velocity dispersion $\sigma(v_r)$                       | $11.4 \pm 1 \text{ km s}^{-1}$     |
| angular extent in $(l, b)$                              | $8^\circ \times 3^\circ$           |
| half-mass radius  | 0.55 kpc                           |
| mean metallicity $\langle [\text{Fe}/\text{H}] \rangle$ | $\sim -1. \text{ dex}$             |

Zhao (1998), where Sagittarius was scattered onto its current tightly bound orbit by an encounter with the Magellanic Clouds about 2 Gyr ago. This appears physically possible but requires careful tuning of the orbits of the two systems.

Driven by this apparent puzzle, we decided to search more thoroughly for a self-consistent model of the disruption of Sagittarius, which, after a Hubble time, has similar characteristics to those observed. (See Table 1 for a summary of the observed properties of the system.) Below we present two models which meet these requirements.

## 2 METHOD

In our numerical simulations, we represent the Galaxy by a fixed potential with three components: a dark logarithmic halo

$$\Phi_{\text{halo}} = v_{\text{halo}}^2 \ln(r^2 + d^2), \quad (1)$$

a Miyamoto-Nagai disk

$$\Phi_{\text{disk}} = -\frac{GM_{\text{disk}}}{\sqrt{R^2 + (a + \sqrt{z^2 + b^2})^2}}, \quad (2)$$

and a spherical Hernquist bulge

$$\Phi_{\text{bulge}} = -\frac{GM_{\text{bulge}}}{r + c}, \quad (3)$$

where  $d=12$  kpc and  $v_{\text{halo}} = 131.5$  km s<sup>-1</sup>;  $M_{\text{disk}} = 10^{11} M_{\odot}$ ,  $a = 6.5$  kpc and  $b = 0.26$  kpc;  $M_{\text{bulge}} = 3.4 \times 10^{10} M_{\odot}$  and  $c = 0.7$  kpc. This choice of parameters gives a flat rotation curve with an asymptotic circular velocity of 186 km s<sup>-1</sup>.

We represent the satellite galaxy by a collection of  $10^5$  particles and model their self-gravity by a multipole expansion of the internal potential to fourth order (White 1983; Zaritsky & White 1988). This type of code has the advantage that a large number of particles can be followed in a relatively small amount of computer time. Hence a substantial parameter space can be explored while retaining considerable detail on the structure of the disrupted system. In this quadrupole expansion, higher than monopole terms are softened more strongly. We choose  $\epsilon_1 \sim 0.2 - 0.25r_c$  for the monopole term ( $r_c$  is the core radius of the system) and  $\epsilon_2 = 2\epsilon_1$  for dipole and higher terms and for the centre of expansion. The centre of expansion is a particle which, in practice, follows the density maximum of the satellite closely at all times.

For the stellar distribution of the pre-disruption dwarf we choose a King model (King 1966), since this is a good representation of the distant dwarf spheroidals. King models are defined by a combination of three parameters:  $\Psi(r=0)$  (depth of the potential well of the system),  $\sigma^2$  (measure of the central velocity dispersion), and  $\rho_0$  (central density) or  $r_0$  (King radius). The ratio  $\Psi(r=0)/\sigma^2$  defines how centrally concentrated the system is, and for any value of this parameter, a set of homologous models with different central densities and core (or King) radii may be found. We assume that the progenitor of Sagittarius obeys the known metallicity-luminosity relation for the Local Group dSph (Mateo 1998). The metallicity determinations for Sagittarius (I97) indicate  $\langle [\text{Fe}/\text{H}] \rangle \sim -1$ , corresponding to a *total* luminosity in the range  $3.5 \times 10^7 - 3.5 \times 10^8 L_{\odot}$ . To obtain an initial guess for the mass of the system, we transform this luminosity into a mass assuming a mass-to-light ratio  $\sim 2$ . The relevant initial stellar mass interval is then  $7 \times 10^7 - 7 \times 10^8 M_{\odot}$ .

Note that our choice of a fixed potential to represent our Galaxy means that we neglect any exchange of energy between the satellite and the Galactic halo. This is an excellent approximation for the range of orbits and satellite masses that we consider, since these imply dynamical friction decay times substantially in excess of the Hubble time. The orbits are also sufficiently large that impulsive heating during disk passages can be neglected.

The orbit of Sagittarius is relatively well constrained (I97). The heliocentric distance  $d \sim 25 \pm 2$  kpc and position

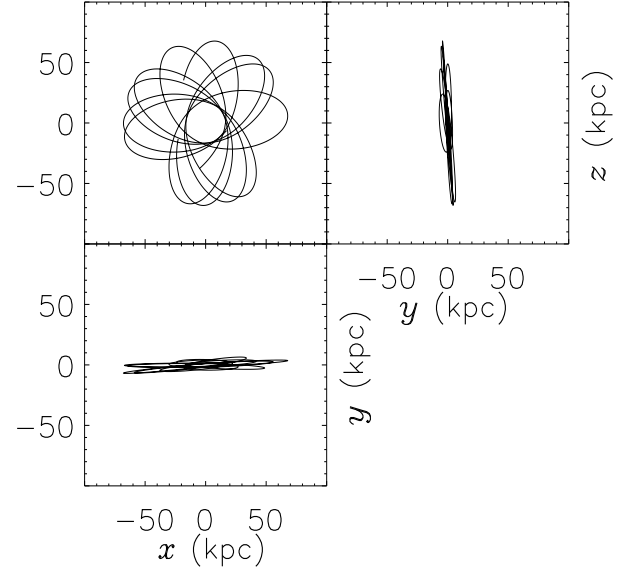


**Figure 1.** Projections of a possible orbit of Sagittarius on different orthogonal planes, where  $xy$  coincides with the plane of the Galaxy.

( $l, b$ ) = ( $5.6^\circ, -14^\circ$ ) of the galaxy core are well-determined; the heliocentric radial velocity  $v_r^{\text{sun}} \sim 140 \pm 2$  km s<sup>-1</sup>, and its variation across the satellite are also accurately measured. Outside the main body ( $b < -20^\circ$ ) the radial velocity shows a small gradient  $dv_r/db \lesssim 3$  km s<sup>-1</sup> deg, but no gradient is detected across the main body itself. The proper motion measurements are not very accurate;  $\mu_b \sim 2.1 \pm 0.7$  mas yr<sup>-1</sup>, and no measurement is available in the  $l$ -direction. On the other hand the strong North-South elongation of the system suggests that it has little motion in the  $l$ -direction. We generate a range of possible orbits satisfying these constraints and concentrate on those with relatively long periods in order to maximise the survival chances of our satellite. We begin all our simulations half a radial period after the Big Bang to allow for the initial expansion. We place the initial satellite at apocentre, then we integrate forward until  $\sim 13$  Gyr. The orbits are chosen so at this time the position and velocity of the satellite core correspond to those observed. We allow ourselves some slight freedom in choosing the final time in order to fit the observed data as well as possible.

## 3 RESULTS

Figure 1 gives an example of an orbit which is consistent with all the current data on Sagittarius. It has a pericentre of 16.3 kpc, an apocentre of 68.3 kpc, and a radial period of  $\sim 0.85$  Gyr.

After letting our satellite relax in isolation, we integrate each simulation for  $\sim 13$  Gyr. In practice we needed to run a large number of simulations, and test each to see if it satisfies the observational constraints at the present time. Since it remains uncertain whether dwarf spheroidals have extended dark halos, we have considered both purely stellar models

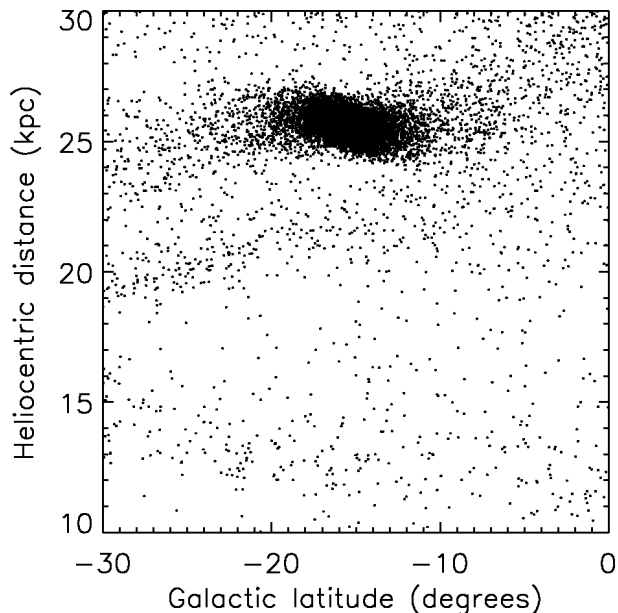


**Figure 2.** Distribution of particles in distance from the Sun as a function of latitude. For direct comparison see Figure 4 of I97.

and models in which the initial stellar system is embedded in a more massive and more extended dark halo.

### 3.1 Constant mass-to-light ratio: A purely stellar model

Our preferred purely stellar model (Model I) initially has a core radius of  $r_c = 0.56$  kpc, a total velocity dispersion of  $18.1 \text{ km s}^{-1}$ , and a concentration parameter  $c = \log_{10}(r_t/r_c) \sim 0.83$ . This implies a total mass of  $M = 5.74 \times 10^8 M_\odot$ . For a satellite to survive for about 10 Gyr on an orbit with pericentre  $\sim 15$  kpc, apocentre  $\sim 70$  kpc, and period  $\sim 1$  Gyr (for which the observational constraints are satisfied) its initial central density has to be  $\rho_0 \geq 0.25 - 0.3 M_\odot \text{ pc}^{-3}$ . Satellites with significantly smaller initial densities do not survive long enough.

In Figure 2 we plot heliocentric distance as a function of galactic latitude for stars projected near the main remnant 12.5 Gyr after infall. Streams of particles are visible at all latitudes over a broad range in distance. Sagittarius has been orbiting long enough for its debris streams to be wrapped several times around the Galaxy. (See also Figure 6.)

The remnant galaxy, i.e. the central region of the satellite’s debris, is similar to the real system. In Figure 3 we plot its mass surface density. The transformation from observed surface brightness to mass surface density (which is what the simulations give us) can be done as follows. The observed mass surface density  $\Sigma$  for an assumed mass-to-light ratio  $\Upsilon$  is

$$\Sigma = \frac{N_X L_X}{f_X} \Upsilon \left[ \frac{M_\odot}{\text{deg}^2} \right], \quad (4)$$

where  $N_X$  is the number of observed stars of type  $X$  per square degree,  $L_X$  is their luminosity, and  $f_X$  is the fraction of the total luminosity in stars of type  $X$ . In IGI95 the spatial structure of Sagittarius was determined from the excess

of counts at apparent magnitude of the horizontal branch. Uncertainties in the result are due primarily to contamination by sources in the Galactic bulge. Their lowest isodensity contour is at  $\Sigma_{\min} \sim 5 \times 10^5 \frac{M_\odot}{\text{deg}^2}$ , assuming  $\Upsilon \sim 2.25$  and  $[\text{Fe}/\text{H}] \sim -1$  (Bergbusch & vandenBerg 1992), and has an extent of  $7.5^\circ \times 3^\circ$ . This same isodensity contour is shown in Figure 3 as a thick line. It has an extent of  $\sim 8^\circ \times 4^\circ$ , in reasonable agreement with the observations given the uncertainties. In I97 isodensity contours were derived from counts of main sequence stars close to the turn-off, roughly one magnitude above the plate limit. The minimum contour in this case corresponds to  $\Sigma_{\min} \sim 10^5 \frac{M_\odot}{\text{deg}^2}$ , and has an extent of roughly  $15^\circ \times 7^\circ$ . In Fig. 3 this contour is shown as a dashed-line, and has an extent of  $15^\circ \times 5.5^\circ$ , also in good agreement with the observations. Note that the isophotes (or isodensity contours) become rounder towards the centre of the satellite. Its angular core radius is  $R_c \sim 1.24^\circ$ , which for a distance of 25.6 kpc (derived from the simulations) corresponds to 0.55 kpc, again in good agreement with the observations.

The kinematic properties of the remnant galaxy are more difficult to compare with observations because a substantial amount of mass from debris streams is projected on top of the main body. Like I97, we measure the radial velocity across the system considering only particles for which  $100 \text{ km s}^{-1} \leq v_r^{\text{sun}} \leq 180 \text{ km s}^{-1}$ . In the left panel of Figure 4 we plot the heliocentric radial velocity, and in the right panel we plot its dispersion as a function of Galactic latitude. For comparison, we analysed the observations of I97 at CTIO in the same way (their Table 2b); these data have a precision of a few  $\text{km s}^{-1}$  (triangles in Figure 4). Our model is consistent with the observed kinematics; we obtain a heliocentric radial velocity of  $138 \text{ km s}^{-1}$  and an internal velocity dispersion in the radial direction of  $10.3 \text{ km s}^{-1}$  for the main body. However, when the radial velocity restrictions for inclusion in this calculation are relaxed, we find much larger velocity dispersions because of the contribution of stars from other streams. It is important to consider this problem when determining which stars should be considered members of Sagittarius.

### 3.2 Varying mass-to-light ratio: A model with a dark halo

The observational data for Sagittarius mainly refer to the current remnant system, which corresponds to the innermost regions of the progenitor satellite. As a consequence, models that are initially dark matter dominated in their outskirts are relatively poorly constrained.

As an example we focus on a progenitor with a mass distribution which is similar to that of Model I in its inner regions but is more extended. We choose the mass-to-light ratio of satellite material to be a decreasing function of binding energy, so that the most bound particles have near “stellar” mass-to-light ratios, whereas weakly bound particles are almost entirely “dark”. We take the initial mass distribution to be a King model with  $r_c = 0.7$  kpc and  $r_t = 13.2$  kpc. For an orbit like that of Model I this produces a suitable remnant after 12 Gyr for an initial total velocity dispersion of  $17.5 \text{ km s}^{-1}$ , giving a total initial mass of  $M = 1.26 \times 10^9 M_\odot$ . The *mass* distribution of this remnant

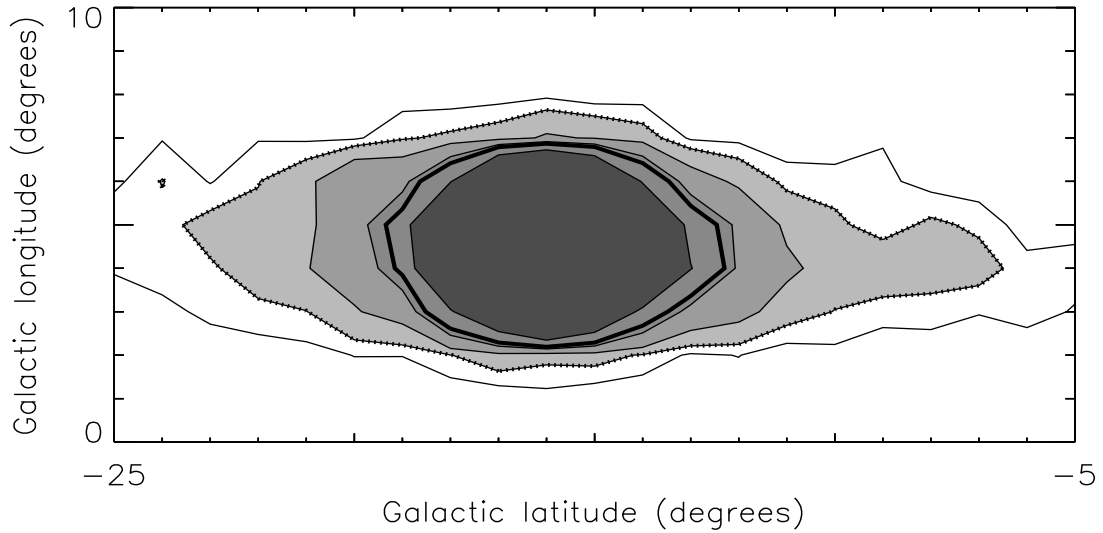


**Figure 3.** Surface isodensity contours for the remnant system. The thick and dashed lines indicate the contours that, for  $M/L = 2.25$ , would correspond to the minimum contours plotted in 1994 and in 1997 respectively by Ibata and collaborators. Each succeeding contour has half the mass surface density of the previous one.

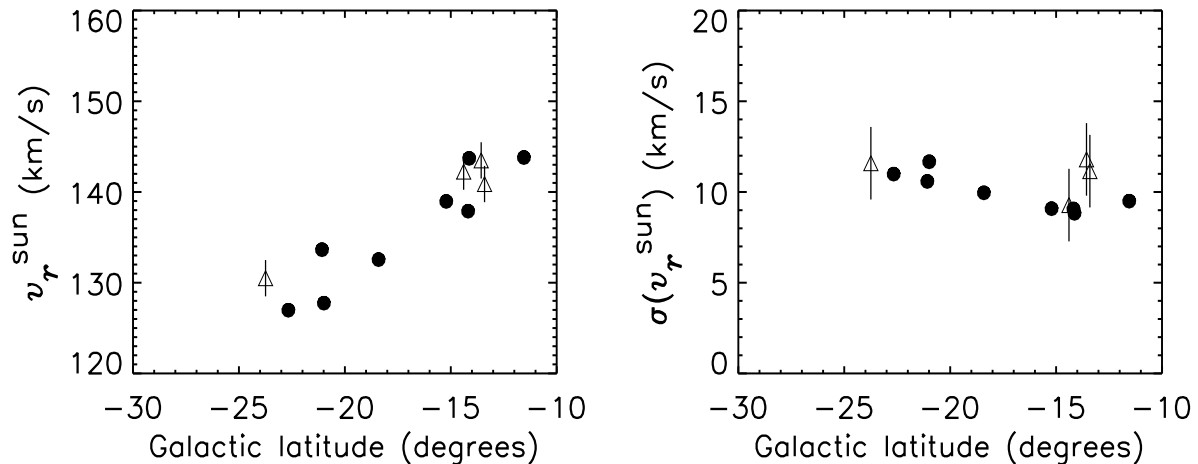


**Figure 4.** In the left panel we plot mean heliocentric radial velocity as a function of Galactic latitude, for bins of  $\sim 2.5^\circ \times 2.5^\circ$  across the remnant system. The right panel shows the heliocentric radial velocity dispersion in the same bins. To determine variations across the main body of the galaxy, we have taken bins centered on the same Galactic latitude but offset in Galactic longitude. The triangles correspond to data from I97, error bars indicate  $2 \text{ km s}^{-1}$  uncertainty.

satisfies many of the observational constraints of Table 1. Its angular core radius is slightly larger  $R_c \sim 1.24^\circ$ , and the radial velocity dispersion in the main body is  $12.5 \text{ km s}^{-1}$ . We construct a two-component satellite with this mass distribution by solving for the dependence of mass-to-light ratio on initial binding energy that produces an initial light profile which is approximately a King model with  $r_c = 0.56 \text{ kpc}$  and  $r_t = 2.44 \text{ kpc}$ . If we identify the central mass-to-light ratio of this system as the “stellar” value, its total to stellar

mass ratio is 6. In fact this is a lower limit, since there must be some dark matter also at the centre of the system.

The actual value of the central mass-to-light ratio is chosen so that the central surface brightness of the remnant agrees with that of Sagittarius. This requires  $\Upsilon = 3.25$ . The total luminosity of the initial model is then  $6.87 \times 10^7 L_\odot$ , implying a mass-to-light ratio of 18.3. We shall refer to this model as Model II. We can calculate its “observable” properties by weighting each simulation particle by  $(M/L)^{-1}$ . Thus

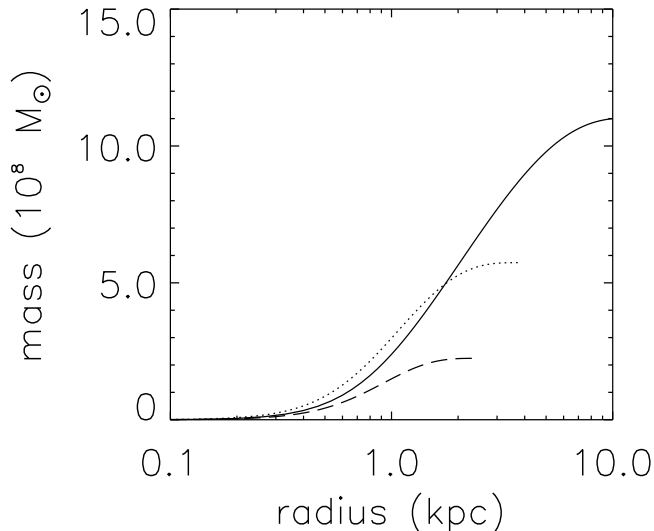


**Figure 5.** Mass profile for Model II (solid curve) and for its “luminous” component (dashed curve). Also shown is the mass profile for Model I (dotted curve).

we find its initial velocity dispersion to be  $17.5 \text{ km s}^{-1}$ , and the velocity dispersion of the remnant to be  $12.8 \text{ km s}^{-1}$ . The visible extent of the remnant is also slightly smaller than the extent of its mass leading to properties which are almost identical to those of Model I and in good agreement with the observations.

Figure 5 compares the initial mass distribution of Model II with the distribution of its light, and with the mass distribution of Model I. Light has been converted to mass using the central mass-to-light ratio; the result thus overestimates the “actual” stellar mass as noted above. The two initial models clearly have very similar mass distributions in their inner regions, a consequence of the requirement that these regions should remain (just) bound after 12.5 Gyr. Although, by construction, the main body of the remnants is very similar in the two cases, there is a significant difference in the properties of their debris streams. In Model I the unbound debris streams are predicted to contain 7.9 times the light in the main body of the remnant ( $M_V \sim -13.8$ ), as defined by the dotted contour in Figure 3, whereas in Model II ( $M_V \sim -14.5$ ) this ratio is 0.24. If we had chosen Model II to be a constant mass-to-light ratio model with the same central value as before, we would have got an almost equally good fit to the main body of Sagittarius, but would have predicted this ratio to be 8.2. In this last case, Sgr would have contributed  $5 \times 10^8 L_\odot$  to the Galactic stellar halo in the form of debris stars (for  $\Upsilon = 2.25$ ). Thus we see that the observed properties of the main remnant do not usefully constrain the number of stars that may be present in the debris streams, but that the different models can be better constrained from the properties of their debris streams.

### 3.3 Discussion

In this section we focus for simplicity on Model I. We can use it to predict where streams originating in different mass loss events should be found. This is illustrated in Figure 6 where

different colours indicate material lost at different pericentric passages. Note that since the surface brightness of the unbound material decreases with time, material lost in early passages is considerably more difficult to detect than recent mass loss (for an axisymmetric potential the time dependence is  $1/t^2$ , but if the potential may be considered as nearly spherical the surface density will effectively decrease as  $1/t$ ; see Helmi & White 1999). The central panel (latitude vs. heliocentric distance) explains why Sagittarius streams have been detected below the Galactic plane but never above it. From the left panel,  $-90^\circ \leq l \leq 90^\circ$ , we see that the stream of stars lost in the previous pericentric passage (shown in blue) becomes more distant as we go north. For example, at  $b = 40^\circ$ , the stream is located approximately 50 kpc from the Sun. The red giant clump visual magnitude at this distance would be roughly  $19.3^m$ , compared to the  $17.85^m$  observed in the main body of Sagittarius. Unfortunately, the observations reported in the literature at this Galactic latitude, either do not reach this magnitude limit, or are offset by a few degrees from the expected location. Thus, for example, Majewski et al. (1999) have a limiting magnitude of 21 at  $b = 41^\circ$  and  $l = -6^\circ$ , but the actual stream in our model is predicted to go through  $l \sim 2^\circ$  and to be about  $2^\circ$  wide. Note that the width prediction is more secure than the location since the motion of Sagittarius in the  $l$ -direction is poorly constrained at present. It is also interesting to note that Majewski and collaborators claimed to detect a Sagittarius stream at  $b = -40^\circ$  and  $l = 11^\circ$ , at a slightly smaller heliocentric distance of 23 kpc and with a radial velocity of the order of  $30 \text{ km s}^{-1}$ . As they discuss, this velocity may be strongly affected by contamination by other Galactic components. We note, however, that we would predict a stream of stars (shown in blue) going through this latitude and longitude with roughly the observed distance, and with a radial velocity of  $54 \text{ km s}^{-1}$ . (See the central and bottom left panels of Fig. 6,  $-90^\circ \leq l \leq 90^\circ$ ). This agreement is encouraging. As mentioned above, this stream is formed by material lost in the previous pericentric passage and not three passages ago, as in the model of Johnston et al. (1999). This difference reflects the different orbital timescales in the two models. The surface density of stars may be able to distinguish between them; it is predicted to be higher in our case.

Our model can also be used to predict star counts as a function of distance and radial velocity at different points on the sky. This is illustrated in Figure 7, where the number counts are normalized to their values on the main body of our simulated Sagittarius, as shown in the first row. We assume fields which are  $5^\circ \times 5^\circ$ . For the distance, we use 5 kpc bins, whereas for the radial velocity we take  $25 \text{ km s}^{-1}$  bins. Note that the contrast of structures in the radial velocity counts are generally larger than in the distance counts, indicating that it should be easier to detect streams in velocity space rather than as density inhomogeneities (see also Helmi & White 1999). This is particularly true considering the much greater relative precision of the velocity measurements. Space density enhancements often occur near the orbital turning points; several are seen as sharp features in the central panel of Fig. 6.

A possible progenitor of Sagittarius could thus be a satellite with a core radius of about 0.56 kpc, a central  $M/L$  ratio of 2.25 and a total stellar velocity dispersion of about

$18 \text{ km s}^{-1}$ . We have found viable models with a wide range of total luminosities and masses, and both with and without extended dark halos. The data available at present only weakly constrain the total initial extent either of the light or of the mass. The observed metallicity data, for example, are consistent with an initial galaxy similar to either of our detailed models, both of which would lie within the scatter of the luminosity–size–velocity dispersion–metallicity distribution for more distant dwarf spheroidal galaxies in the Local Group. Thus we see no indication that Sagittarius is in any way anomalous. Further work on the debris streams of Sagittarius is needed to constrain better its initial total luminosity, and to distinguish between purely stellar or dark-matter dominated progenitors.

## REFERENCES

- Bergbusch P.A., Vandenberg D.A., 1992, *Ap. J. Suppl.*, 81, 163  
 Edelson D.J., Elmegreen B.G., 1997, *MNRAS*, 290, 7  
 Helmi A., White S.D.M., 1999, *MNRAS*, 307, 495  
 Ibata R., Gilmore G., Irwin G., 1994, *Nature*, 370, 194  
 Ibata R., Gilmore G., Irwin G., 1995, *MNRAS*, 277, 781 (IG195)  
 Ibata R., Wyse R.F.G., Gilmore G., Irwin G., Suntzeff, N.B. 1997, *AJ*, 113, 634 (I97)  
 Ibata R., Lewis G.F., 1998, *ApJ*, 500, 575  
 Johnston K.V., Spergel D.N., Hernquist L., 1995, *ApJ*, 451, 598  
 Johnston K.V., Hernquist L., Bolte M., 1996, *ApJ*, 465, 278  
 Johnston K.V., Majewski S.R., Siegel M.H., Kunkel W.E., 1999, *AJ*, 118, 1719  
 King I.R., 1966, *AJ*, 71, 64  
 Majewski S.R., Siegel M.H., Kunkel W.E., Reid I.N., Johnston K.V., Thompson I.B., Landolt A.U., Palma C., 1999, *AJ*, 118, 1709  
 Mateo M., 1998, *ARA&A*, 36, 435  
 Mateo M., Olszewski E.W., Morrison H.L., 1998, *ApJ*, 508, L55  
 Velázquez H., White S.D.M., 1995, *MNRAS*, 275, 23L  
 White S.D.M., 1983, *ApJ*, 274, 53  
 Zaritsky D., White S.D.M., 1988, *MNRAS*, 235, 289  
 Zhao H.S., 1998, *ApJ*, 500, L149

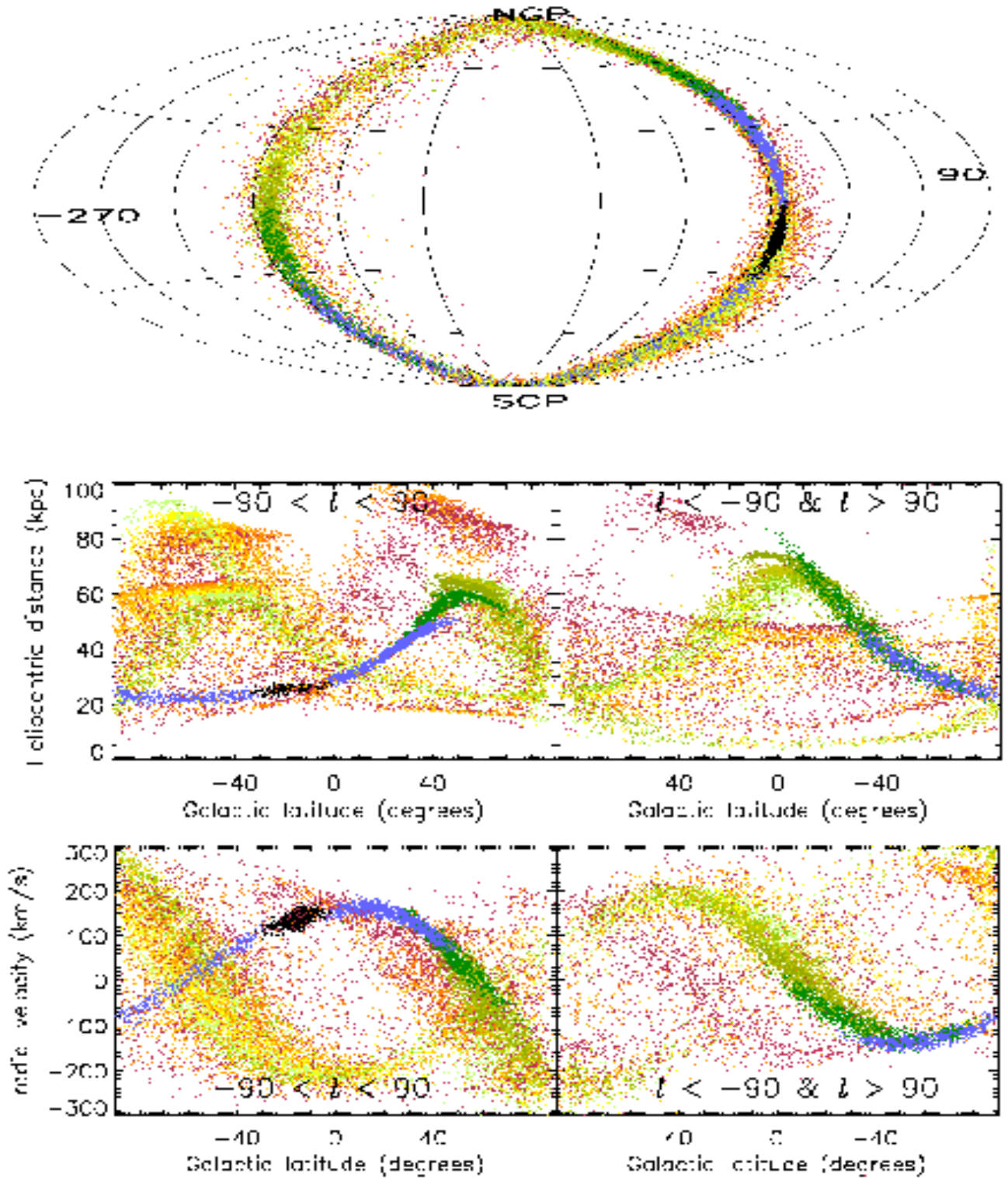


**Figure 6.** **Top panel:** Distribution in the sky ( $l, b$ ) of the particles for our constant mass-to-light ratio model of Sagittarius after 12.5 Gyr. Different colors indicate material stripped off in different passages. **Central panel:** Heliocentric distance as a function of Galactic latitude, at the same time as the top panel, and with the same colour coding. Note that “streams” formed early on are wider than the more recent ones. **Bottom panel:** Heliocentric radial velocity as a function of Galactic latitude, at the same time and using the same colour coding as before.

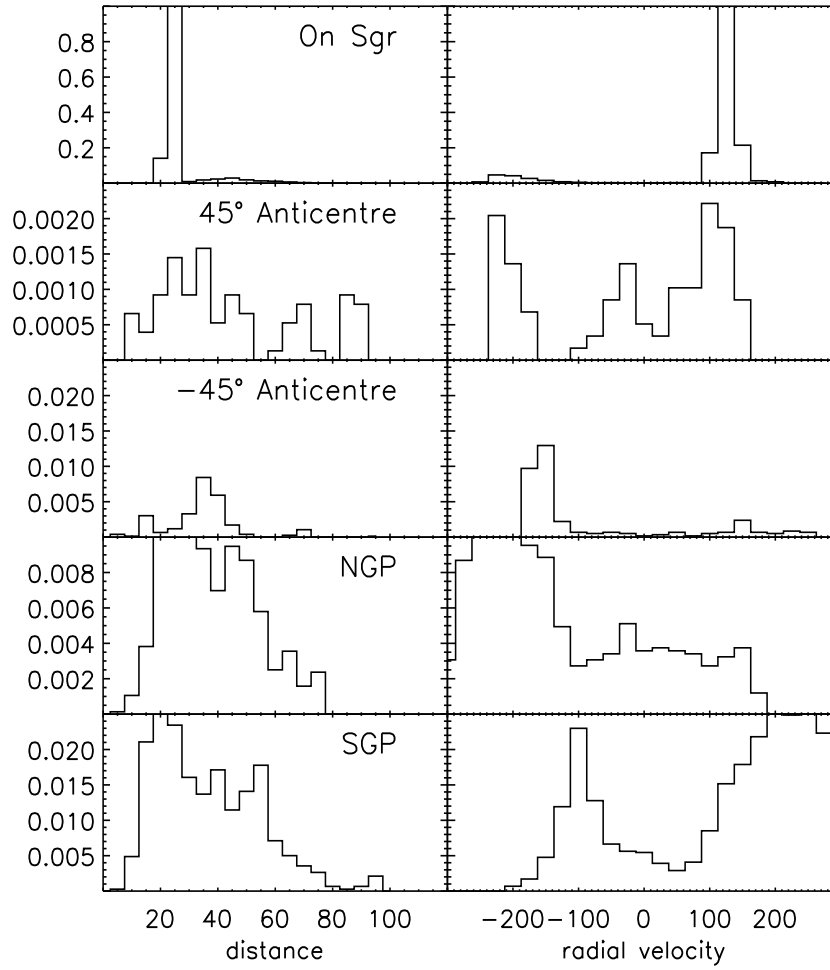


**Figure 7.** Number counts in  $5 \times 5 \text{ deg}^2$  normalized to the main body of Sagittarius, which is shown in the top row. Distance bins are 5 kpc, and radial velocity bins are  $25 \text{ km s}^{-1}$ . All quantities are heliocentric.